MEMBERSHIP IN THE REGION OF THE OPEN CLUSTER NGC 2244

B. E. Sabogal-Martínez, J. A. García-Varela, M. A. Higuera G.,
A. Uribe, and E. Brieva

Observatorio Astronómico Nacional, Facultad de Ciencias,
Universidad Nacional de Colombia

RESUMEN

Se construye un modelo bivariado doble elíptico para determinar la pertenencia de estrellas en la región del cúmulo abierto NGC 2244. Se realiza un ajuste a la secuencia principal de edad cero o ZAMS y se determina su módulo de distancia.

ABSTRACT

A double elliptic bivariate model has been developed to solve the membership problem in the region of the open cluster NGC 2244. Once the physical cluster members were found a fit to the ZAMS was made in order to find the NGC 2244 distance modulus.

Key Words: **METHODS: STATISTICAL — OPEN CLUSTERS AND ASSOCIATIONS: INDIVIDUAL (NGC 2244) — STARS: DISTANCES**

1. INTRODUCTION

The cluster NGC 2244 is located at the center of the H II region NGC 2237–2247, known as the Rosette nebula. Its equatorial coordinates for 1950's are: $\alpha = 6^{\mathrm{h}}29.7^{\mathrm{m}}$; $\delta = 4°54'$. This young cluster with a 4.8 magnitude has a relatively high brightness, an approximate radius of 11.8 pc and an age of 3×10^6 yr (Marschall, Van Altena, & Chiu 1982).

NGC 2244 has been the subject of several photometric and astrometric studies; in a very important one made by Marschall et al. (1982), the proper motions of 287 stars of the cluster region with $V \leq 14.00$ were published and membership probabilities were assigned from an analysis of the distribution of the proper motions, following the method of Chiu & Van Altena (1981) and Cudworth (1976). The proper motions reported in the former paper have been used in the present work to calculate the membership probabilities of the stars in the NGC 2244 cluster region, working with a model analogous to that proposed by Vasilevskis, Klemola, & Preston (1958) and Vasilevskis (1962); but now we model the distribution of the proper motion of the cluster stars through a circular normal bivariate probability density function, and the proper motions of the field stars by an elliptic normal bivariate probability density function.

The proper motion distribution by Marschall et al. (1982) shows a strong elongation parallel to the y axis observed in the VPD or vector point diagram of the proper motions. Applying the Sanders (1971) methodology to the usual nine parameter model we did not find an acceptable solution for the generated maximum likelihood equation system. Therefore, we have built a new proper motion distribution model, using elliptic normal bivariate density functions for both the cluster and the field, and so introducing new parameters for the cluster distribution, as will be explained in the next section.

2. MEMBERSHIP PROBABILITIES

The discrimination between members of the field and members of the cluster is based on a double elliptic model obtained from a contagious or mixed bivariate proper motions probability density function given by the

following equation

$$
\begin{aligned}
\Phi(\mu_x, \mu_y) \;=\; & (1 - n_f)\Phi_c(\mu_x, \mu_y) + n_f \Phi_F(\mu_x, \mu_y) \\[2mm]
=\; & \frac{1 - n_f}{2\pi\sigma_{xc}\sigma_{yc}\sqrt{1 - \rho_c^2}} \exp\left\{ -\frac{1}{2(1-\rho_c^2)}\left[\begin{array}{l} \left(\frac{\mu_x - \mu_{x0c}}{\sigma_{xc}}\right)^2 + \left(\frac{\mu_y - \mu_{y0c}}{\sigma_{yc}}\right)^2 \\ -2\rho_c\left(\frac{\mu_x - \mu_{x0c}}{\sigma_{xc}}\right)\left(\frac{\mu_y - \mu_{y0c}}{\sigma_{yc}}\right) \end{array} \right] \right\} \\[2mm]
+\; & \frac{n_f}{2\pi\sigma_{xf}\sigma_{yf}\sqrt{1 - \rho_f^2}} \exp\left\{ -\frac{1}{2(1-\rho_f^2)}\left[\begin{array}{l} \left(\frac{\mu_x - \mu_{x0f}}{\sigma_{xf}}\right)^2 + \left(\frac{\mu_y - \mu_{y0f}}{\sigma_{yf}}\right)^2 \\ -2\rho_f\left(\frac{\mu_x - \mu_{x0f}}{\sigma_{xf}}\right)\left(\frac{\mu_y - \mu_{y0f}}{\sigma_{yf}}\right) \end{array} \right] \right\}.
\end{aligned}
\tag{1}
$$

This probability density function is not normal, and depends on eleven parameters: $\mu_{x0c}, \mu_{y0c}, \mu_{x0f}, \mu_{y0f}$, the cluster and the field proper motions centroids; $\sigma_{xc}, \sigma_{yc}, \sigma_{xf}, \sigma_{yf}$, the dispersions or standard deviations for the cluster and the field proper motions; n_f, the proportion of field stars; and ρ_f and ρ_c, the cluster and the field proper motions correlation coefficients.

When a mixture model is built overlapping two normal elliptic bivariate density functions instead of overlapping just a circular one and an elliptic bivariate component, two new dispersion parameters, σ_{xc} and σ_{yc}, appear in the equation of the model; they replace the dispersion parameter of a circular bivariate model for the cluster, σ_c. At the same time a new correlation parameter ρ_c is defined.

The function given in equation (1) satisfies the condition

$$
\int_{-\infty}^{\infty}\int_{-\infty}^{\infty} \left[(1 - n_f)\Phi_c(\mu_x, \mu_y) + n_f \Phi_f(\mu_x, \mu_y)\right] \, d\mu_x \, d\mu_y \;=\; 1.
\tag{2}
$$

2.1. Maximum Likelihood Equations

The model parameters are the components of the vector $\vec{\theta}$

$$
\vec{\theta} = (\mu_{x0f}, \mu_{y0f}, \sigma_{xf}, \sigma_{yf}, \mu_{x0c}, \mu_{y0c}, \sigma_{xc}, \sigma_{yc}, n_f, \rho_f, \rho_c).
\tag{3}
$$

They are estimated using a maximum likelihood method (Sanders 1971), that gives a system of eleven coupled non linear equations where the index i refers to the star number; the associated parameter is given on the left side of each equation.

μ_{x0f} :
$$
\sum_{i=1}^{N} \left\{ \frac{n_f}{2\pi\sigma_{xf}\sigma_{yf}\sqrt{1 - \rho_f^2}} \right\} \left\{ \frac{\mu_{xi} - \mu_{x0f}}{\left(1 - \rho_f^2\right)\sigma_{xf}^2} - \frac{\rho_f\,(\mu_{yi} - \mu_{y0f})}{\left(1 - \rho_f^2\right)\sigma_{xf}\sigma_{yf}} \right\} \Phi_i^{-1}A_i = 0 \,,
\tag{4}
$$

μ_{y0f} :
$$
\sum_{i=1}^{N} \left\{ \frac{n_f}{2\pi\sigma_{xf}\sigma_{yf}\sqrt{1 - \rho_f^2}} \right\} \left\{ \frac{\mu_{yi} - \mu_{y0f}}{\left(1 - \rho_f^2\right)\sigma_{yf}^2} - \frac{\rho_f\,(\mu_{xi} - \mu_{x0f})}{\left(1 - \rho_f^2\right)\sigma_{xf}\sigma_{yf}} \right\} \Phi_i^{-1}A_i = 0 \,,
\tag{5}
$$

σ_{xf} :
$$
\sum_{i=1}^{N} \left\{ \frac{n_f \Phi_i^{-1}A_i}{2\pi\sigma_{xf}^2\sigma_{yf}\sqrt{1 - \rho_f^2}} \right\} \left\{ \frac{1}{\left(1 - \rho_f^2\right)}\left(\frac{\mu_{xi} - \mu_{x0f}}{\sigma_{xf}}\right)^2 - \frac{\rho_f\,(\mu_{xi} - \mu_{x0f})\,(\mu_{yi} - \mu_{y0f})}{\left(1 - \rho_f^2\right)\sigma_{xf}\sigma_{yf}} - 1 \right\} = 0 \,,
\tag{6}
$$

$\sigma_{yf}:$

$$\sum_{i=1}^{N} \left\{ \frac{n_f \Phi_i^{-1} A_i}{2\pi\sigma_{yf}^2 \sigma_{xf}\sqrt{1-\rho_f^2}} \right\} \left\{ \begin{array}{l} \frac{1}{(1-\rho_f^2)} \left(\frac{\mu_{yi}-\mu_{y0f}}{\sigma_{yf}}\right)^2 - \\ \frac{\rho_f \ (\mu_{xi}-\mu_{x0f}) \ (\mu_{yi}-\mu_{y0f})}{(1-\rho_f^2) \ \sigma_{xf}\sigma_{yf}} \ - \ 1 \end{array} \right\} = 0 \ , \tag{7}$$

$\mu_{x0c}:$

$$\sum_{i=1}^{N} \left\{ \frac{1-n_f}{2\pi\sigma_{xc}\sigma_{yc}\sqrt{1-\rho_c^2}} \right\} \left\{ \frac{\mu_{xi}-\mu_{x0c}}{(1-\rho_c^2) \ \sigma_{xc}^2} - \frac{\rho_c \ (\mu_{yi}-\mu_{y0c})}{(1-\rho_c^2) \ \sigma_{xc}\sigma_{yc}} \right\} \Phi_i^{-1} B_i = 0 \ , \tag{8}$$

$\mu_{y0c}:$

$$\sum_{i=1}^{N} \left\{ \frac{1-n_f}{2\pi\sigma_{xc}\sigma_{yc}\sqrt{1-\rho_c^2}} \right\} \left\{ \frac{\mu_{yi}-\mu_{y0c}}{(1-\rho_c^2) \ \sigma_{yc}^2} - \frac{\rho_c \ (\mu_{xi}-\mu_{x0c})}{(1-\rho_c^2) \ \sigma_{xc}\sigma_{yc}} \right\} \Phi_i^{-1} B_i = 0 \ , \tag{9}$$

$\sigma_{xc}:$

$$\sum_{i=1}^{N} \left\{ \frac{(1-n_f) \ \Phi_i^{-1} B_i}{2\pi\sigma_{xc}^2 \sigma_{yc}\sqrt{1-\rho_c^2}} \right\} \left\{ \begin{array}{l} \frac{1}{(1-\rho_c^2)} \left(\frac{\mu_{xi}-\mu_{x0c}}{\sigma_{xc}}\right)^2 - \\ \frac{\rho_c \ (\mu_{xi}-\mu_{x0c}) \ (\mu_{yi}-\mu_{y0c})}{(1-\rho_c^2) \ \sigma_{xc}\sigma_{yc}} \ - \ 1 \end{array} \right\} = 0 \ , \tag{10}$$

$\sigma_{yc}:$

$$\sum_{i=1}^{N} \left\{ \frac{(1-n_f) \ \Phi_i^{-1} B_i}{2\pi\sigma_{yc}^2 \sigma_{xc}\sqrt{1-\rho_c^2}} \right\} \left\{ \begin{array}{l} \frac{1}{(1-\rho_c^2)} \left(\frac{\mu_{yi}-\mu_{y0c}}{\sigma_{yc}}\right)^2 - \\ \frac{\rho_c \ (\mu_{xi}-\mu_{x0c}) \ (\mu_{yi}-\mu_{y0c})}{(1-\rho_c^2) \ \sigma_{xc}\sigma_{yc}} \ - \ 1 \end{array} \right\} = 0 \ , \tag{11}$$

$n_f:$

$$\sum_{i=1}^{N} \left\{ \frac{A_i}{2\pi\sigma_{xf}\sigma_{yf}\sqrt{1-\rho_f^2}} - \frac{B_i}{2\pi\sigma_{xc}\sigma_{yc}\sqrt{1-\rho_c^2}} \right\} \Phi_i^{-1} = 0 \ , \tag{12}$$

$\rho_f:$

$$\sum_{i=1}^{N} \left\{ \frac{n_f \Phi_i^{-1} A_i}{2\pi\sigma_{xf}\sigma_{yf}\left(1-\rho_f^2\right)^{\frac{5}{2}}} \right\} \left\{ \begin{array}{l} \rho_f \ (1-\rho_f^2) + \\ \left(1+\rho_f^2\right) \left(\frac{\mu_{xi}-\mu_{x0f}}{\sigma_{xf}}\right) \left(\frac{\mu_{yi}-\mu_{y0f}}{\sigma_{yf}}\right) \\ - \ \rho_f \ \left\{ \left(\frac{\mu_{xi}-\mu_{x0f}}{\sigma_{xf}}\right)^2 + \left(\frac{\mu_{yi}-\mu_{y0f}}{\sigma_{yf}}\right)^2 \right\} \end{array} \right\} = 0 \ , \tag{13}$$

$\rho_c:$

$$\sum_{i=1}^{N} \left\{ \frac{(1-n_f) \ \Phi_i^{-1} B_i}{2\pi\sigma_{xc}\sigma_{yc}\left(1-\rho_c^2\right)^{\frac{5}{2}}} \right\} \left\{ \begin{array}{l} \rho_c \ (1-\rho_c^2) + \\ \left(1+\rho_c^2\right) \left(\frac{\mu_{xi}-\mu_{x0c}}{\sigma_{xc}}\right) \left(\frac{\mu_{yi}-\mu_{y0c}}{\sigma_{yc}}\right) \\ - \ \rho_c \ \left\{ \left(\frac{\mu_{xi}-\mu_{x0c}}{\sigma_{xc}}\right)^2 + \left(\frac{\mu_{yi}-\mu_{y0c}}{\sigma_{yc}}\right)^2 \right\} \end{array} \right\} = 0 \ , \tag{14}$$

where

$$A_i = \exp\left\{ -\frac{1}{2\left(1-\rho_f^2\right)} \left\{ \left(\frac{\mu_{xi}-\mu_{x0f}}{\sigma_{xf}}\right)^2 + \left(\frac{\mu_{yi}-\mu_{y0f}}{\sigma_{yf}}\right)^2 \right\} \right\} \times \exp\left\{ \frac{1}{\left(1-\rho_f^2\right)} \left\{ \rho_f \ \frac{(\mu_{xi}-\mu_{x0f}) \ (\mu_{yi}-\mu_{y0f})}{\sigma_{xf}\sigma_{yf}} \right\} \right\} \tag{15}$$

$$B_i = \exp\left\{ -\frac{1}{2\left(1-\rho_c^2\right)} \left\{ \left(\frac{\mu_{xi}-\mu_{x0c}}{\sigma_{xc}}\right)^2 + \left(\frac{\mu_{yi}-\mu_{y0c}}{\sigma_{yc}}\right)^2 \right\} \right\} \times \exp\left\{ \frac{1}{(1-\rho_c^2)} \left\{ \rho_c \ \frac{(\mu_{xi}-\mu_{x0c}) \ (\mu_{yi}-\mu_{y0c})}{\sigma_{xc}\sigma_{yc}} \right\} \right\} \tag{16}$$

$$\Phi_i^{-1} = \frac{1}{\Phi_i} \, . \tag{17}$$

It is important to note that in the previous equations both correlation terms, ρ_f and ρ_c, were included and that they were not eliminated by rotation to a preferential reference frame.

Once the equations system has been solved, a Bayes rule can be followed in order to assign cluster membership probabilities P_i working from the estimated mixed probability density function

$$P_i \left(C|\mu_{xi}, \mu_{yi}\right) = \frac{n_c \; \Phi_c \left(\mu_{xi}, \mu_{yi}\right)}{n_c \; \Phi_c \left(\mu_{xi}, \mu_{yi}\right) + n_f \; \Phi_F \left(\mu_{xi}, \mu_{yi}\right)} . \tag{18}$$

A star is considered a cluster member if the membership probability found is grater than or equal to 0.5 (Bayes minimum error rate of misclasification) (Cabrera & Alfaro 1990; Uribe & Brieva 1994).

2.2. *Initial Parameter Estimation*

The equation system (4) to (14) was solved numerically using the ZSYSTM routine and assigning initial parameter values as a starting point. This routine is an IMSL Fortran code that solves a system of non linear equations. It implements the Brown method solution (Hiebert 1982), a modification of Newton's method which tries to improve some aspects concerned with efficiency, uses Gauss elimination, and gives the solution of the non linear system; its main advantage is local quadratic convergence.

Though we have certainly experienced that the method is somewhat sensitive to variations of the starting parameter estimations, only unreasonable initial values cause divergence. Therefore, we can claim that a local maximum for the likelihood function is found close to the automatic starting point proposed.

Sanders (1971) suggested some initial parameter values, and he found that they were applicable to virtually all the cases that he examined, once extreme data or outliers were pruned out. We took advantage of that astronomical experience and realized that very similar starting values could be obtained by an automatic two step procedure developed on a reasonable statistical basis that takes into account an exploratory data analysis and the spread of the field proper motion as the first step. The second step was designed to virtually prune out the outliers and gives weight to the greater concentration of the proper motions of the cluster stars.
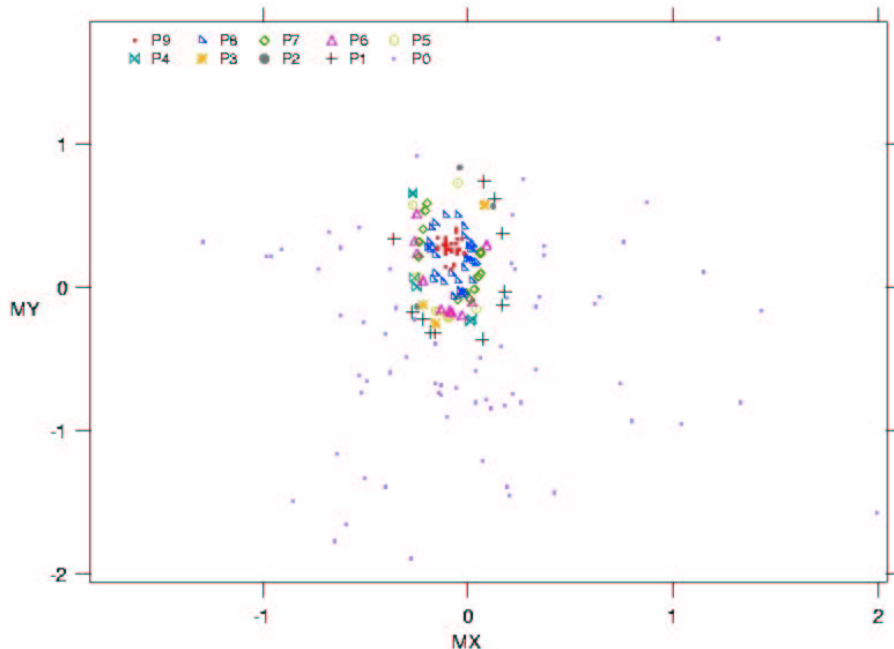

Fig. 1. VPD of the cluster NGC 2244 taking into account the membership probabilitiy classes.

First, the proper motion histograms, μ_x and μ_y are built and next a Gaussian function is fit to each histogram. The Gaussian functions that fit the μ_x and μ_y data are given by

$$f_x = A \exp\left\{ -\frac{1}{2}\left(\frac{\mu_x - \mu_{x0}}{\sigma_{x0}}\right)^2 \right\}, \tag{19}$$

$$f_y = B \exp\left\{ -\frac{1}{2}\left(\frac{\mu_y - \mu_{y0}}{\sigma_{y0}}\right)^2 \right\}. \tag{20}$$

Once we know the values of μ_{x0}, μ_{y0}, σ_{x0}, and σ_{y0}, we obtain initial values for the parameters of the density function that model the field. Thus we have: $\mu_{x0f} = \mu_{x0}$; $\mu_{y0f} = \mu_{y0}$; $\sigma_{xf} = 2\sigma_{x0}$; $\sigma_{yf} = 2\sigma_{y0}$. The initial proportion of field stars is fixed to the value $n_f = 0.5$; the initial correlations are given by $\rho_f = \rho_c = 0.0150$.

Then, in a second step, new Gaussian adjustments to the histograms of μ_x and μ_y are made, but in this case the range of the proper motions is respectively, limited to the intervals $[\mu_{x0} - \sigma_{x0}, \mu_{x0} + \sigma_{x0}]$ and $[\mu_{y0} - \sigma_{y0}, \mu_{y0} + \sigma_{y0}]$. The new functions are given by

$$f'_x = C \exp\left\{ -\frac{1}{2}\left(\frac{\mu_x - \mu'_{x0}}{\sigma'_{x0}}\right)^2 \right\}, \tag{21}$$

$$f'_y = D \exp\left\{ -\frac{1}{2}\left(\frac{\mu_y - \mu'_{y0}}{\sigma'_{y0}}\right)^2 \right\}. \tag{22}$$

Thus, the remaining four starting parameter values are: $\mu_{x0c} = \mu'_{x0}$; $\mu_{y0c} = \mu'_{y0}$; $\sigma_{xc} = \frac{\sigma'_{x0}}{4}$; $\sigma_{yc} = \frac{\sigma'_{y0}}{4}$.
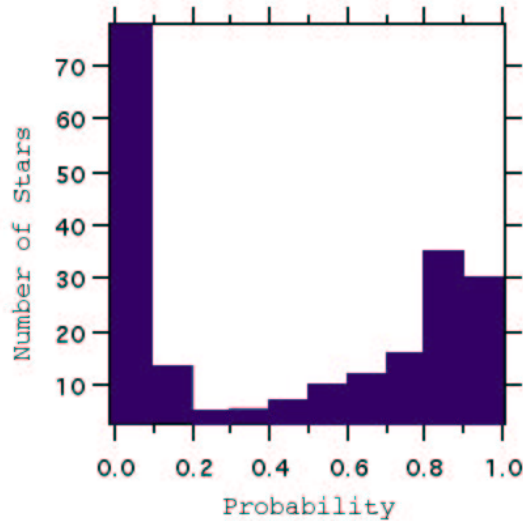
Fig. 2. Membership probabilities histogram for the cluster NGC 2244.

3. RESULTS

From the list of the stars with proper motions published by Marschall et al. (1982), 192 of quality class 9 and 10 were chosen; 26 of them were excluded as outliers. The stars with membership probabilities $P < 0.5$ were 74, and the stars with $P \geq 0.5$ were 92. Therefore, 92 stars were considered as physical members of the cluster NGC 2244. The maximun likelihood parameter estimations found are given in Table 1.
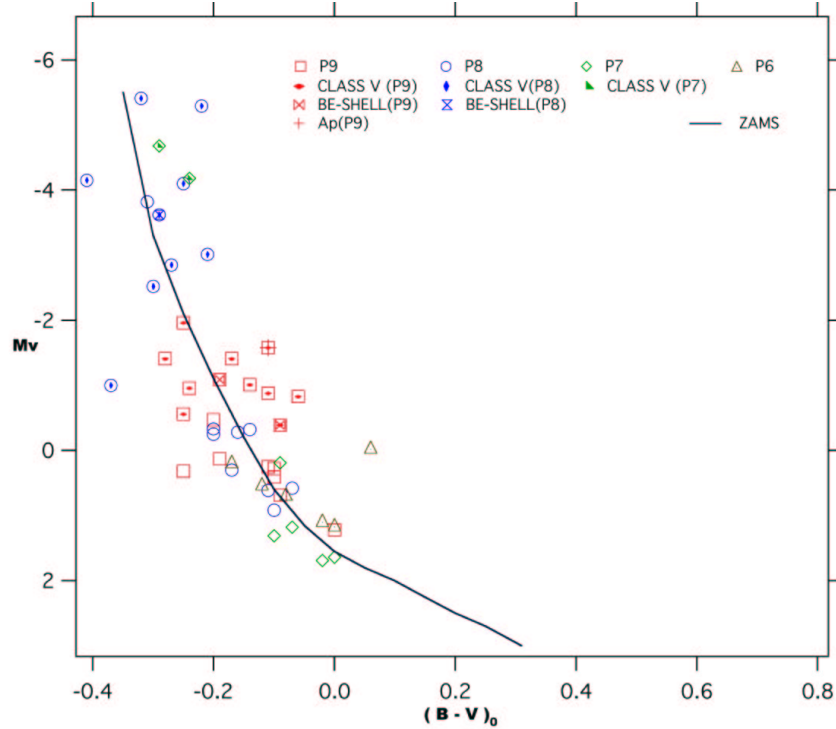
Fig. 3. CM or color magnitude diagram for the type V stars, Be-shell stars, and Ap stars of the cluster NGC 2244.

The VPD of proper motions is shown in Figure 1, where the nine probability classes given in Table 2 have been plotted. In this VPD we clearly see the elliptic distribution of the proper motions of the cluster stars around a centroid and the very small dispersion for the stars with probability classes between P7 and P9; the dispersion is a little greater for the stars with probabilities between P0 and P6. The proper motions of the stars in the field region show a greater dispersion than the proper motions of the stars in the cluster.

The U shaped probability histogram shown in Figure 2 proves the power of the method to discriminate the cluster and the field, and allows only small uncertainties in this discrimination.

In Table 3 we list the 192 stars. The first column is our identification number. The second column gives the identification number for the photometric study of Ogura & Ishida (1981), used also by Marschall et al. (1982). The next two columns are the relative proper motions in arcseconds per century taken from Marschall et al. (1982). The fifth column lists the membership probabilities according to our study. The last column gives the membership probabilities found by Marschall et al. (1982) working from proper motions.

There is a nice agreement with the work on proper motions made by Baumgardt, Dettbarn, & Wielen (2000) as concerns the open cluster NGC 2244. We also found that the stars 115, 114, 122, 203 are cluster members and we have rejected the star 266 just as they did using information provided by *Hipparcos* (parallax and proper motion). Our data did not include the stars 400 and 387 considered by them as non-members, and the star 389 that they ascribed to the cluster as a probable member with a low membership probability value equal to 0.502. The previous numbers are from the BDA or Data Base for Galactic open clusters, and are the same that are given by Ogura & Ishida (1981) and Marschall et al. (1982); they appear in the ID2 column of the Table 3.

3.1. *NGC 2244 Color Magnitude Diagram and Distance Modulus*

The photometric data for 50 of the 92 cluster members were obtained from Marschall et al. (1982); the information for $B - V$, V, and E_{B-V} has the following errors: $\Delta B - V = 0.01^{\mathrm{m}}$, $\Delta V = 0.01^{\mathrm{m}}$, and $\Delta E_{B-V} =$

TABLE 1

VALUES FOR THE ELEVEN PARAMETERS
OF THE CONTAGIOUS MODEL

Parameter	Initial Value	Solution Value
μ_{x0f}	-0.0381	-0.064707
μ_{y0f}	0.1656	-0.086165
σ_{xf}	0.4057	0.369333
σ_{yf}	0.5600	0.463687
μ_{x0c}	-0.1200	-0.080605
μ_{y0c}	0.2000	0.199977
σ_{xc}	0.0806	0.091055
σ_{yc}	0.0992	0.208046
n_f	0.5000	0.511713
ρ_f	0.0150	-0.067306
ρ_c	0.0150	-0.158787

TABLE 2

PROBABILITY CLASSES

Probability Class	Interval
P0	$0.0 \leq P < 0.1$
P1	$0.1 \leq P < 0.2$
P2	$0.2 \leq P < 0.3$
P3	$0.3 \leq P < 0.4$
P4	$0.4 \leq P < 0.5$
P5	$0.5 \leq P < 0.6$
P6	$0.6 \leq P < 0.7$
P7	$0.7 \leq P < 0.8$
P8	$0.8 \leq P < 0.9$
P9	$0.9 \leq P < 1.0$

0.01^{m}. To find $(B-V)_0$ and V_0 the value $R_V = 3.2 \pm 0.01$ was used (Ogura & Ishida 1981). Based on these data the cluster distance modulus was found through a ZAMS fit (Blaauw 1963), taking only into account the cluster members. The value $V - M_V = 10.70 \pm 0.04$ that we obtained is in a very good agreement with the one reported by Ogura & Ishida (1981).

Once the $(B-V)_0$ and M_V values were obtained from the ZAMS fit a color magnitude plot was made (Figure 3). The overlap of the cluster main sequence with the ZAMS of Blaauw is shown. The wide dispersion of the main sequence stars may be explained by differential extinction in that region, in agreement also with the 2 to 3 magnitudes variation found for R_V (Marschall et al. 1982). This effect was not taken into account to obtain the V_0 and $(B-V)_0$ values; they were calculated from an average value for $R_V = 3.2$ (Ogura & Ishida 1981).

4. CONCLUSIONS

The method built to find the initial starting parameter values leads to a solution of the maximum likelihood equations; furthermore, it allows us to find those values avoiding personal and subjective criteria, and makes it easier to find parameter estimates. The method and the model proposed have proved to be efficient to discriminate between the two populations (cluster and field stars) in the region of the cluster NGC 2244. The U shaped histogram of the membership probabilities found underlines the suitability of the model.

The elliptic double model constructed to calculate the NGC 2244 cluster membership probabilities was able to discriminate between the stars of the field and the stars of the cluster, in agreement with the results obtained by Baumgardt et al. (2000) and by Marschall et al. (1982) who assigned 110 stars to the cluster, from proper motions and a different model. This supports the validity and reliability of the elliptic double model, that could be applied to solved the membership problem in those cases where the VPD of proper motions shows a preferential direction, as in the case of the cluster NGC 2244.

The distance modulus found in the paper by Ogura & Ishida (1981) was 10.76 ± 0.07 magnitudes. They used photometric membership probabilities greater or equal than 0.9. The agreement of our work with this result is another way to prove that the double elliptic model leads to reliable results when solving the membership problem.

TABLE 3

OBSERVATIONAL PROPER MOTION DATA AND MEMBERSHIP
PROBABILITIES FOR NGC 2244

ID1	ID2	μ_x	μ_y	P1	P2	ID1	ID2	μ_x	μ_y	P1	P2
1	2	−0.590	−1.650	0.00	0.00	48	114	0.030	−0.010	0.76	0.95
2	8	−0.400	−0.320	0.00	0.00	49	115	−0.010	−0.040	0.79	0.93
3	9	−0.300	−0.480	0.00	0.00	50	116	−0.150	0.280	0.90	0.90
4	11	−0.650	−1.770	0.00	0.00	51	118	−0.160	−0.310	0.18	0.24
5	12	−0.100	−0.900	0.00	0.00	52	120	−0.530	0.420	0.00	0.00
6	14	0.220	−0.740	0.00	0.97	53	122	−0.120	0.040	0.85	0.86
7	16	0.870	0.600	0.00	0.00	54	123	−0.220	−0.220	0.18	0.17
8	18	0.110	−0.840	0.00	0.01	55	124	0.010	−0.230	0.47	0.80
9	20	0.130	0.620	0.11	0.98	56	125	−0.160	0.230	0.88	0.87
10	25	−0.160	−0.670	0.00	0.01	57	127	0.070	−0.360	0.12	0.61
11	29	0.020	−0.100	0.68	0.91	58	128	−0.020	0.140	0.89	0.97
12	30	0.330	−0.130	0.00	0.00	59	129	0.020	−0.220	0.47	0.82
13	31	1.990	−1.570	0.00	0.00	60	130	−0.110	0.270	0.91	0.94
14	32	−0.640	−1.160	0.00	0.00	61	131	−0.260	0.070	0.49	0.31
15	35	−0.160	−0.250	0.30	0.34	62	133	−0.120	0.300	0.91	0.94
16	36	−0.180	−0.310	0.14	0.18	63	135	−0.060	−0.700	0.00	0.02
17	39	−0.220	−0.120	0.37	0.29	64	136	−0.040	0.840	0.27	0.97
18	40	0.160	−0.410	0.02	0.42	65	140	−0.380	0.130	0.04	0.02
19	41	−0.280	−1.890	0.00	0.00	66	142	−0.490	−0.650	0.00	0.00
20	42	−0.910	0.270	0.00	0.00	67	156	−1.290	0.320	0.00	0.00
21	44	−0.070	0.160	0.91	0.95	68	158	−0.400	−1.390	0.00	0.00
22	45	0.010	−0.080	0.72	0.92	69	160	−0.250	0.240	0.69	0.52
23	46	−0.240	0.320	0.74	0.62	70	163	−0.980	0.220	0.00	0.00
24	47	−0.380	−0.590	0.00	0.00	71	164	−0.090	−0.160	0.65	0.88
25	48	0.040	−0.150	0.56	0.89	72	167	−0.020	0.240	0.90	0.97
26	53	1.220	1.740	0.00	0.00	73	169	0.190	−0.070	0.09	0.88
27	57	−0.850	−1.490	0.00	0.00	74	171	1.330	−0.800	0.00	0.00
28	67	1.430	−0.160	0.00	0.00	75	172	−0.110	0.350	0.91	0.95
29	69	−0.250	−0.130	0.22	0.16	76	173	0.180	−0.820	0.00	0.01
30	72	−0.130	−0.750	0.00	0.00	77	174	−0.130	−0.150	0.61	0.64
31	74	−0.220	0.050	0.65	0.51	78	175	−0.050	−0.080	0.78	0.88
32	78	−0.160	−0.160	0.51	0.50	79	176	1.150	0.110	0.00	0.00
33	79	−0.110	0.240	0.91	0.94	80	180	−0.080	0.100	0.89	0.93
34	80	−0.010	0.200	0.89	0.97	81	181	0.260	−0.800	0.00	0.00
35	81	−0.250	0.080	0.56	0.37	82	183	0.350	−0.060	0.00	0.41
36	82	−0.240	0.220	0.72	0.56	83	188	0.740	−0.670	0.00	0.00
37	83	−0.270	0.580	0.50	0.49	84	189	−0.100	−0.200	0.55	0.65
38	84	−0.040	−0.020	0.83	0.92	85	190	0.020	0.310	0.85	0.98
39	85	0.070	−1.210	0.00	0.00	86	192	−0.180	0.420	0.86	0.87
40	86	−0.620	−0.190	0.00	0.00	87	193	−0.050	0.260	0.91	0.97
41	90	−0.520	−0.730	0.00	0.00	88	194	−0.110	0.320	0.91	0.95
42	91	0.370	0.230	0.00	0.62	89	195	−0.220	0.410	0.79	0.75

TABLE 3 (CONTINUED)

ID1	ID2	μ_x	μ_y	P1	P2	ID1	ID2	μ_x	μ_y	P1	P2
43	100	−0.130	−0.680	0.00	0.01	90	196	−0.210	0.540	0.75	0.80
44	106	−0.250	0.010	0.46	0.30	91	197	−0.170	0.280	0.88	0.87
45	107	0.200	−1.450	0.00	0.00	92	198	−0.190	0.270	0.85	0.81
46	110	−0.140	−0.160	0.57	0.58	93	200	0.040	0.180	0.82	0.98
47	111	0.620	−0.110	0.00	0.00	94	201	0.000	0.290	0.88	0.98
95	202	−0.060	0.390	0.90	0.97	144	304	1.040	−0.950	0.00	0.00
96	203	0.020	0.050	0.81	0.98	145	305	0.050	0.080	0.77	0.97
97	205	−0.050	0.240	0.91	0.97	146	308	0.170	0.380	0.15	0.98
98	206	−0.050	0.510	0.85	0.98	147	309	0.020	0.190	0.85	0.98
99	207	3.310	−1.930	0.00	0.00	148	311	−0.020	0.430	0.86	0.98
100	210	0.210	0.170	0.07	0.95	149	312	−0.010	−0.040	0.79	0.93
101	212	0.020	0.300	0.85	0.98	150	315	2.030	−1.270	0.00	0.00
102	213	−0.200	0.280	0.84	0.79	151	317	0.630	2.420	0.00	0.00
103	221	−0.040	−0.030	0.82	0.91	152	319	−0.150	0.270	0.90	0.90
104	225	−0.360	0.340	0.13	0.06	153	321	-3.900	1.090	0.00	0.00
105	229	0.760	0.320	0.00	0.00	154	323	−0.080	0.310	0.92	0.96
106	231	−0.160	0.450	0.87	0.91	155	325	−0.200	0.590	0.73	0.83
107	232	0.640	−0.060	0.00	0.00	156	327	−0.250	0.520	0.64	0.62
108	233	−0.140	−0.730	0.00	0.01	157	330	−0.350	−0.140	0.02	0.01
109	234	0.060	−0.490	0.03	0.31	158	331	−0.040	0.270	0.91	0.97
110	235	−0.030	−0.190	0.60	0.81	159	332	0.060	0.100	0.75	0.97
111	236	0.330	−0.570	0.00	0.01	160	333	−0.090	−0.200	0.57	0.68
112	239	−0.060	0.310	0.91	0.97	161	334	−0.090	0.270	0.92	0.96
113	241	−0.080	0.270	0.92	0.96	162	336	0.230	0.130	0.04	0.93
114	242	0.800	−0.930	0.00	0.00	163	337	−0.110	0.290	0.91	0.95
115	245	0.060	0.240	0.77	0.98	164	340	−0.510	−0.240	0.00	0.00
116	249	0.000	0.200	0.88	0.97	165	342	−2.450	0.510	0.00	0.00
117	252	−0.080	−0.170	0.64	0.75	166	343	0.370	0.290	0.00	0.65
118	253	−0.080	0.250	0.92	0.96	167	345	−0.110	0.350	0.91	0.95
119	256	−0.110	0.150	0.90	0.92	168	348	0.030	0.170	0.84	0.97
120	260	−0.260	0.330	0.67	0.51	169	349	−0.150	0.350	0.90	0.92
121	261	−0.620	0.280	0.00	0.00	170	351	0.270	0.760	0.00	0.93
122	262	−0.730	0.130	0.00	0.00	171	352	0.420	−1.430	0.00	0.00
123	263	0.010	0.270	0.87	0.98	172	354	−0.020	0.360	0.88	0.98
124	266	-3.690	0.070	0.00	0.00	173	355	0.170	−0.120	0.11	0.87
125	267	−0.190	0.320	0.86	0.83	174	358	−0.030	−0.050	0.80	0.91
126	268	−0.030	0.340	0.90	0.98	175	362	0.190	−1.390	0.00	0.00
127	271	−0.170	0.060	0.80	0.75	176	363	0.040	−0.800	0.00	0.01
128	274	−0.060	0.410	0.90	0.97	177	364	−0.680	0.390	0.00	0.00
129	276	0.080	0.740	0.13	0.98	178	365	−0.530	−0.610	0.00	0.00
130	277	−0.960	0.220	0.00	0.00	179	372	−0.170	−2.960	0.00	0.00
131	278	0.260	−2.120	0.00	0.00	180	375	−0.160	−0.390	0.08	0.14
132	279	−0.050	0.340	0.91	0.97	181	376	−0.160	0.100	0.85	0.81

TABLE 3 (CONTINUED)

ID1	ID2	μ_x	μ_y	P1	P2	ID1	ID2	μ_x	μ_y	P1	P2
133	280	−0.050	0.270	0.91	0.97	182	377	−0.050	0.050	0.87	0.94
134	281	0.180	−0.030	0.13	0.91	183	379	−.020	−0.030	0.81	0.93
135	282	−0.270	0.660	0.40	0.47	184	380	−0.100	0.300	0.92	0.95
136	283	−0.270	−0.170	0.11	0.08	185	381	−0.080	0.130	0.90	0.94
137	288	−0.070	−0.060	0.80	0.87	186	390	−0.500	−1.330	0.00	0.00
138	291	−0.110	0.510	0.87	0.96	187	391	0.090	−0.780	0.00	0.01
139	292	−0.250	0.920	0.09	0.42	188	393	0.120	0.570	0.20	0.99
140	293	0.220	0.510	0.02	0.97	189	394	0.040	−0.580	0.01	0.14
141	298	0.080	0.580	0.37	0.99	190	396	0.090	0.300	0.64	0.98
142	301	0.020	0.270	0.85	0.98	191	397	−0.050	0.730	0.55	0.97
143	302	0.060	0.250	0.77	0.98	192	402	−0.260	−0.220	0.09	0.07

REFERENCES

Baumgardt, H., Dettbarn, C., & Wielen, R. 2000, A&AS, 146, 246
Blaaw, A. 1963, Stars and Stellar Systems, 3, 383
Cabrera, J., & Alfaro, E. 1990, A&AS, 235, 94
Chiu, L., & Van Altena, W. 1981, AJ, 243, 827
Cudworth, K. 1976, AJ, 81, 519
Hiebert, K. L. 1982, ACM Transactions on Mathematical Software, 8, 5
Marschall, L., Van Altena, W., & Chiu, L. 1982, AJ, 87, 1497
Ogura, K., & Ishida, K. 1981, PASJ, 33, 149
Sanders, W. 1971, A&A, 14, 226
Uribe, A., & Brieva, E. 1994, Ap&SS, 214, 171
Vasilevskis, S. 1962, AJ, 67, 699
Vasilevskis, S., Klemola, A., & Preston, G. 1958, AJ, 63, 387

E. Brieva, J. A. García-Varela, M. A. Higuera G., B. E. Sabogal-Martínez, and A. Uribe: Observatorio Astronómico Nacional, Facultad de Ciencias, Universidad Nacional de Colombia, Ciudad Universitaria, Apartado Postal 2426, Santafé de Bogotá, Colombia (ahiguera, auribe, bsabogal, ebrieva, jgarcia@ciencias.ciencias.unal.edu.co).